ANALYSIS OF THE GRAVITATIONAL-WAVE SIGNAL GW150914

Giovanni Cozzolongo

29 April 2021

Abstract

The gravitational wave signal GW150914 has been analyzed with data from the Laser Interferometer Gravitational-Wave Observatory (LIGO) of Hanford and Livingston. In particular, the evolution of the Amplitude Spectral Density (ASD) of the noise as a function of time has been analyzed for the interferometers that revealed the event. Furthermore, the Power Spectral Density (PSD) of the signal has been realized. This procedure has been performed for each detector and their results have been compared. Finally the bayesian inference was executed to find the median, the 90% credible interval and the correlations of some event's parameters.

Contents

1 Introduction

There are systems consisting of two black holes in a close orbit around each other. One of the mechanisms by which they release energy is the emission of gravitational waves (perturbation of space-time that propagates at the speed of light). The emission of these waves causes the orbit to decay, with a consequent decrease in the orbital period, a step called inspiral. This step is followed by the merging of the black holes, then the amplitude of the gravitational wave reaches its peak. Finally, the settlement occurs, which is known as ringdown.
To detect gravitational waves signals, LIGO Hanford and Livingston, in America, were used. They are a modified Michelson's interferometer, in which a laser is divided into two beams by a beam splitter inclined at 45 degrees. The light propagates in two perpendicular arms with lenght 4 km, reflected by mirrors placed at the ends of the arms and recombined on the beam splitter, generating interference. An incoming gravitational wave changes the optical path of the laser beams in the arms, which then changes the recorded interference pattern.

2 Observation

On September 14th, 2015 at 09:50:45 UTC, the LIGO Hanford and Livingston observatories detected the coincident signal GW150914.

3 Noise analysis of detectors

The ASD of the signal is showed in Fig. 1. An interval of one hour centered around the time of the event was cosidered. It is seen that LIGO-Hanfort is generally more sensitive than LIGO-Livingston at lower frequencies. The shape of the curves is due to many noise sources: for lower frequency seismic noises (earthquakes, wind, ocean waves and human activities) are dominant, then thermal noise in the middle and quantum noise (e.g. shot noise) for the high ones. Various strategies have been adopted to reduce these noises, including insulation from the outside with the help of vacuum and suspension for mirrors and instruments. There are also some narrow-band features like the calibration lines, the vibrational modes of suspension fibers and 60 Hz electric power grid harmonics. For more details see [1].
The time evolution of the ASD at the various fre-

quencies was also analyzed. In particular, frequency intervals of 10 Hz from 10 Hz to 1400 Hz were considered. For each of these, the ASD was averaged in 4-second intervals from 30 minutes before to 30 minutes after the time of the event. The Fig. 3 shows the evolution of all the frequency intervals considered. It can be seen that for some frequency ranges the average of the ASD oscillates around a constant average value. While in some ranges there is an increase or a decrease in the ASD mean. Examples for the latter are the 500-510 Hz and 1000-1010 Hz ranges, which encompass some of the frequencies to which detectors are less sensitive. Indeed a marked downward trend of their average ASDs have been observed in the Fig. 4. This indicates deviations from stationary detector noise.

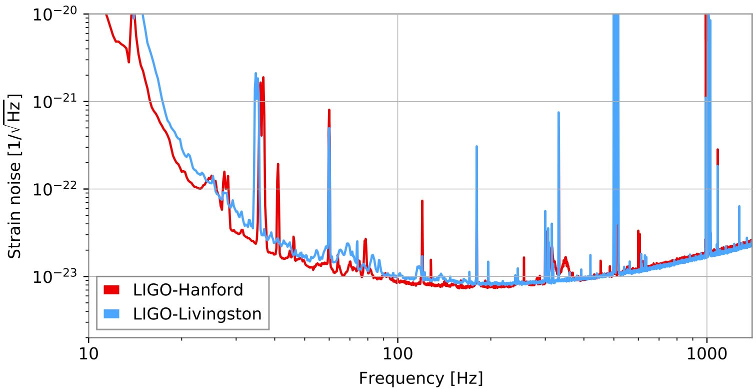

Figure 1: Instrument noise for each detector close to the time of the event detection. The sensitivity is limited by the noise sources described in the text.

4 Quicklook time analysis

The representation of the two detectors time series of strain shows that the signal is more easily visible for LIGO-Hanford than LIGO-Livingston. For making it visible, data are filtered with a 50–300 Hz band-pass filter to suppress large fluctuations outside this range (mostly seismic noise at low frequencies and quantum noise at high frequencies) and band-reject filters (notch) in 60 Hz to remove the electric power spectral line. The results are showed in Fig. 2.

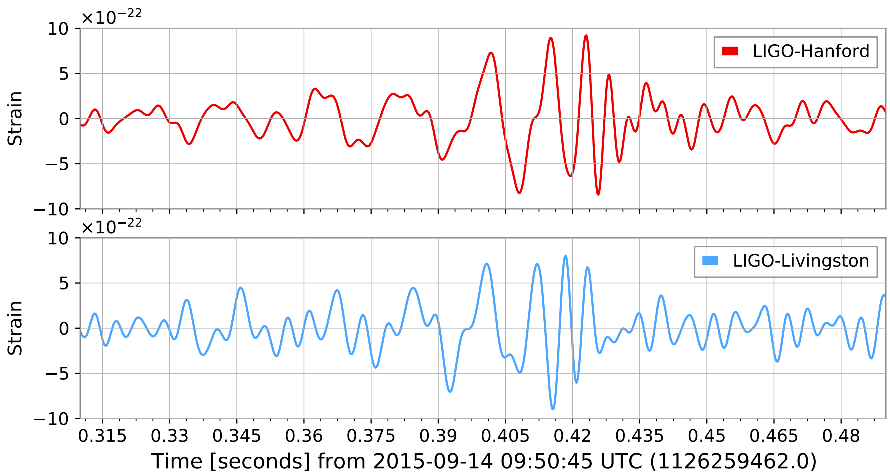

Figure 2: Time series of the strain for LIGO-Hanford (top) and LIGO-Livingston (bottom). The data are filtered by a 50–300 Hz band-pass and a notch in 60 Hz.

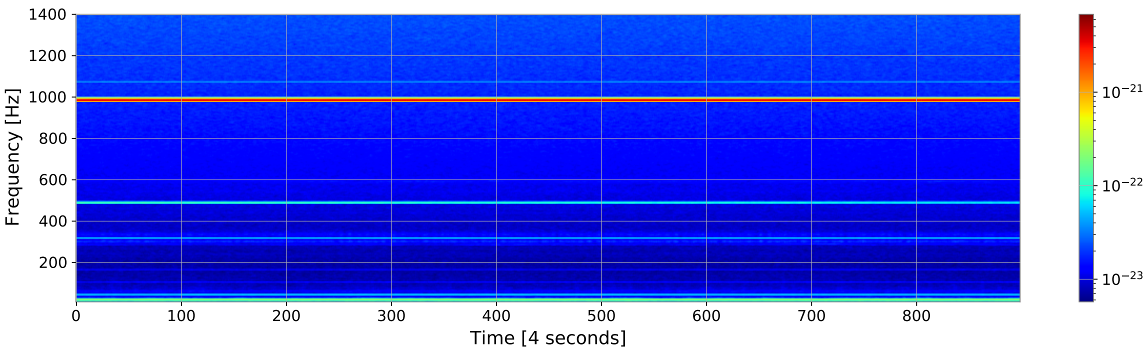

(a) LIGO-Hanford

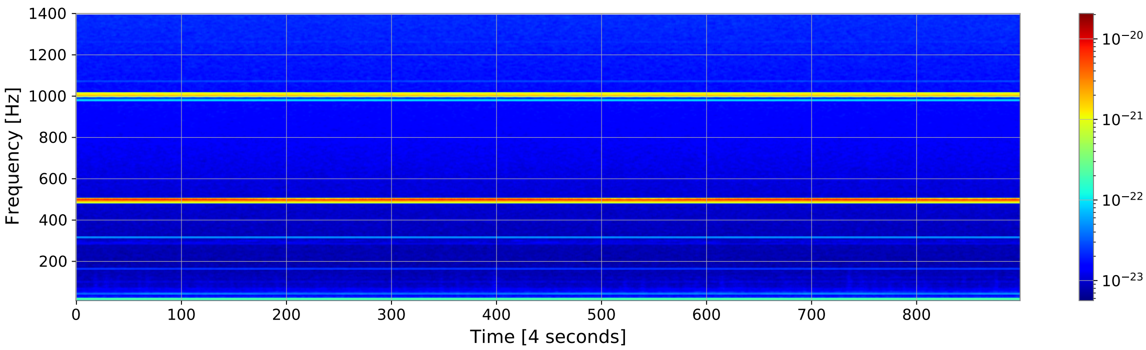

(b) LIGO-Livingston

Figure 3: Time evolution of the instrument noise for each detector. The data are close to the time of event detection.

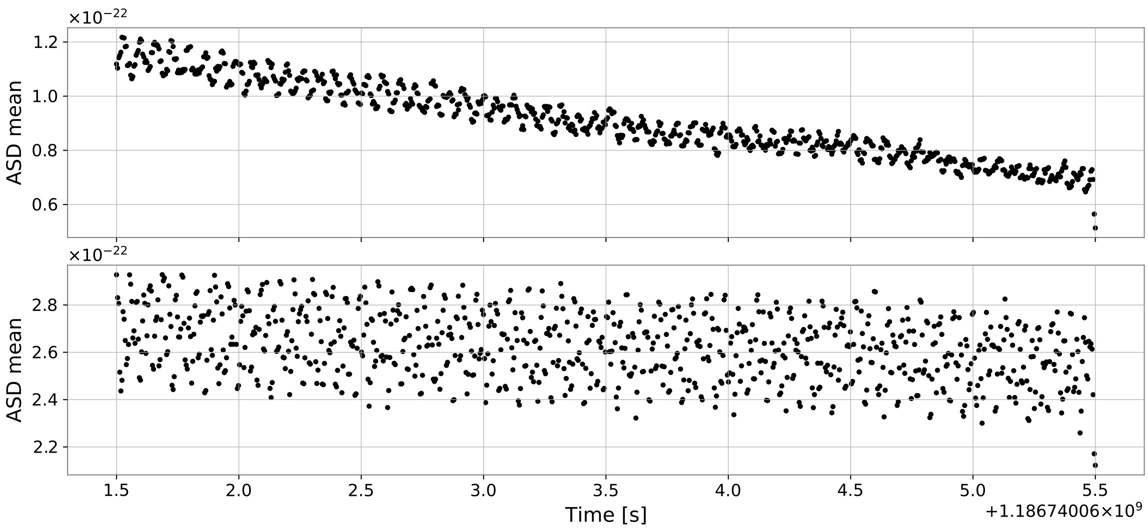

Figure 4: Two examples of instrument noise time evolution for LIGO-Hanford. The top and bottom pannels refer, respectively, to the frequency range 500-510 Hz and 1000-1010 Hz.

5 Signal search

Signal searches with template matching using *PyCBC* have been executed for both detectors. From the data, the frequencies below 15 Hz have been removed and data were downsampled to 2048 Hz. Then both the template and the data have been whitened and the band-pass between $30-300$ Hz were used.

The results are showed in Fig. 5. The used template is SEOBNRv4_opt, which is a model of compact objects pair merge with the masses of each object as parameters. The heavier black hole is called the primary and its label mass is m_1, while the secondary (lighter) black hole is m_2. In particular, the research has been carried out starting from a mass equal to $30\,\mathrm{M}_{\odot}$ for both objects and then various masses were tested, obtained by adding or subtracting the quantity $0.5\,\mathrm{M}_{\odot}$ iteratively to the initial values. Thus, the uncertainty is $0.5\,\mathrm{M}_{\odot}$. From all the attempts, the masses combinations corresponding to the best SNR have been chosen. The results are showed in Tab. 1, where there is also the total mass M_{tot} and chirp mass $\mathcal{M}$, with uncertainties obtained by the propagation of m_1 and m_2 uncertainties. The Chirp mass is defined as

$$\mathcal{M} = \frac{(m_1\, m_2)^{3/5}}{(m_1 + m_2)^{1/5}}.$$

The ratio of the single-detector signal to noise ration (SNR) in LIGO Hanford and Livingston is about 1.5. The SNR difference is predominantly due to the different sensitivities of the detectors.

LIGO-Hanford dected the event after 7 ms resepct to LIGO-Livingston. The two detectors are separated by approximately 3000 km and the gravitational waves propagate at the speed of light, therefore the result is consistent.

In Fig. 5 there are also the power maps of LIGO strain data, made by a Q-transform. Note that there are both the original power maps and the one obtained by subtracting the template. The characteristic upward-chirping morphology of a binary inspiral driven by the gravitational waves emission is visible in both detectors, with a higher signal amplitude in LIGO-Hanford. This is more evident at low frequencies, in according to the analysis of the ASD in Fig. 1.

6 Bayesian inference

To describe the signal of a compact binary coalescense there are many parameters. They describe the masses, spins, orientation, position and time of the merge. From data, it is possible to find the posterior distribution of the parameters with *Bilby*. The template SEOBNRv4_opt were used.

To speed up the analysis, some parameters were fixed to the known values. Furthermore, bayesian inference methods are much faster if the parameters to estimate are not highly correlated. In particular, the Chirp mass and the mass ratio $q = \frac{m_2}{m_1}$ were used, instead of m_1 and m_2. After inferred $\mathcal{M}$ and q, the two masses were found.

The results are shown in Fig. 6 and Tab. 2. In particular, the corner plot shows the correlation between the primary and secondary mass. The values are generally compatible with those obtained with the metched filter.

Finally, the Bayes factor K were found for the signal vs. Gaussian noise. It quantifies the probability that the segment contains a binary black hole signal or just a noise. The result is $\log_{10}(K) = 267.7 \pm 0.1$, which means that the signal hypotesis is strongly supported by the data [2].

7 Conclusions

The ASD for the signal GW150914 has undergone significant changes over time at certain frequencies and the sensitivity of LIGO-Livingstone has been generally the lowest compared to the one of LIGO-Hanford at lower frequencies.

LIGO Livingston was the first to detect the event and did it with a worst SNR than LIGO-Hanford. The signal matches the wave form predicted by general relativity for the inspiral and merger of a pair of black holes and the ring down of the resulting single black hole, using the template SEOBNRv4_opt. The results are compatible with the Bilby analysis.

References

[1] B P Abbott et al 2020, "A guide to LIGO-Virgo detector noise andextraction of transient gravitational-wave signals", Class. Quantum Grav. 37 055002.

[2] Jeffreys, Harold (1998) [1961]. The Theory of Probability (3rd ed.). Oxford, England. p. 432. ISBN 9780191589676.

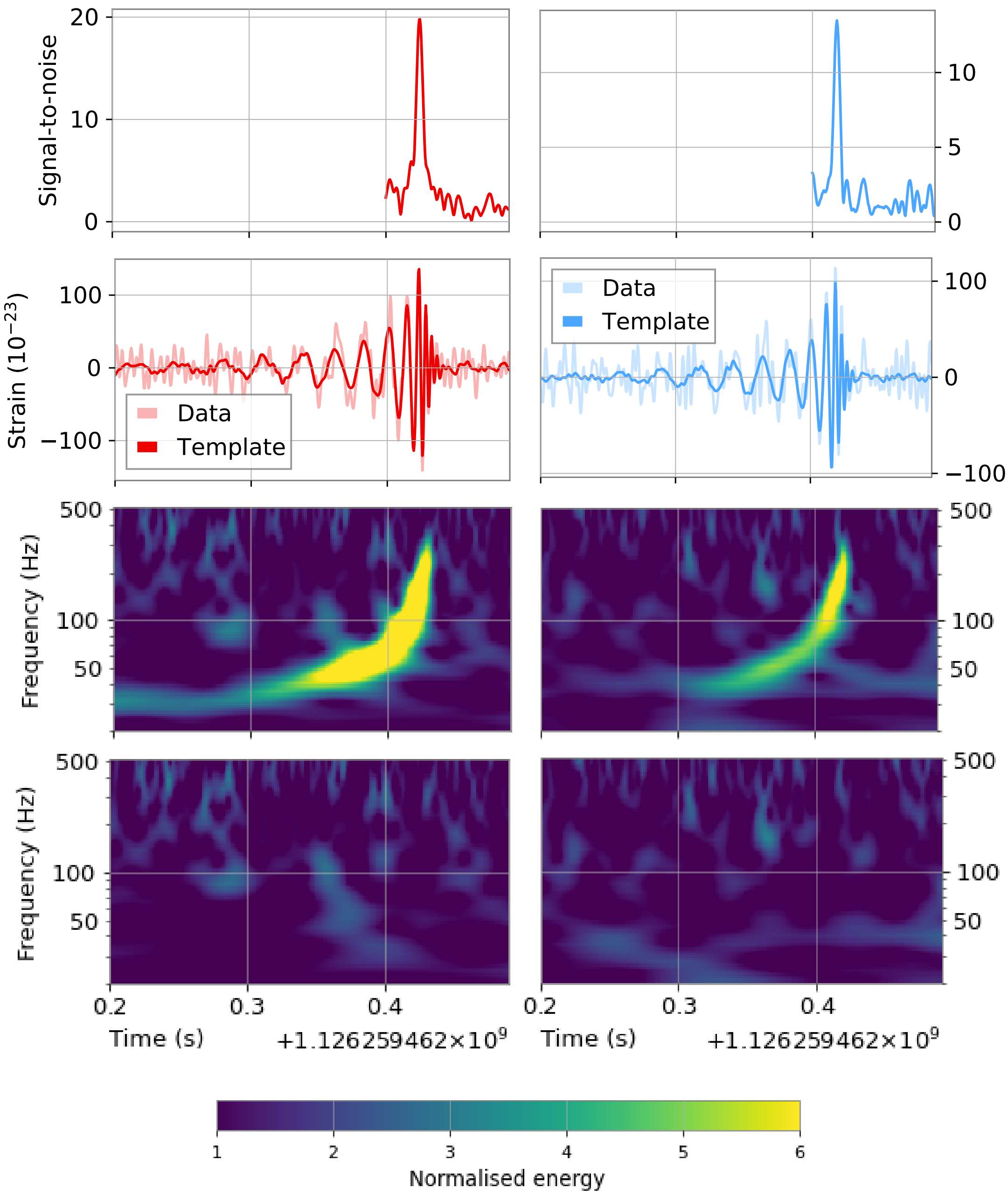

Figure 5: Analysis of data from LIGO-Hanford (left) and LIGO-Livingston (right). Top row: SNR time series. Second row: Time-frequency representation of the strain data and the template of the matched filter. Third row: power maps of strain data by Q-transform. Bottom row: power maps as the previous one, but subtracting the aligned template.

ifo	m_1 [$M_\odot$]	m_2 [$M_\odot$]	M_{tot} [$M_\odot$]	$\mathcal{M}$ [$M_\odot$]	SNR
H1	39.5 ± 0.5	33.0 ± 0.5	72.5 ± 0.7	31.4 ± 0.4	20
L1	39.5 ± 0.5	31.5 ± 0.5	71.0 ± 0.7	30.7 ± 0.4	13.5

Table 1: The results of the matched filter for each detector. Note that ifo is the interferometer identification name, m_1 is the primary mass, m_2 is the secondary mass, M_{tot} is the total mass and $\mathcal{M}$ is the chirp mass.

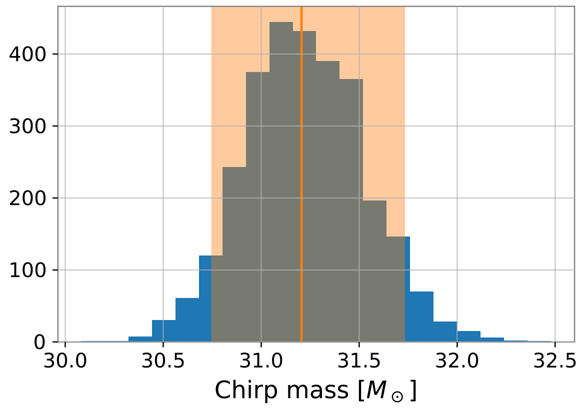

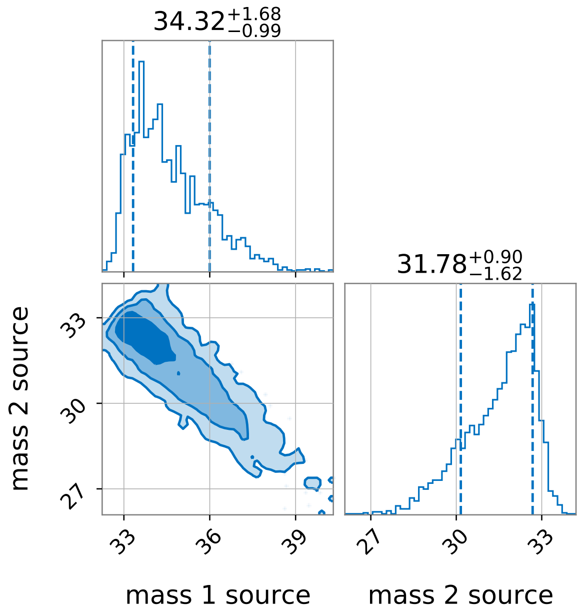

Figure 6: Histogram of the chirp mass with a region to indicate the 90% C.I and line to indicate the median value. (left). Corner plots between m_1 and m_2 (right).

name	med. [$M_\odot$]	90% C.I. [$M_\odot$]
m_1	34.3	32.9 − 37.2
m_2	31.8	29.1 − 33.0
$\mathcal{M}$	31.2	30.7 − 31.7

Table 2: The results of the Bayesian inference. The first column indicates the considered mass, while the second is about the median value. Finally, in the third one there is the 90% credible interval.